

## LASER SPECKLE PHOTOGRAPHY TECHNIQUE FOR MEASURING LOCAL AND GLOBAL HEAT TRANSFER CORRELATION COEFFICIENTS

---

*T. E. Walsh and K. D. Kihm*

*Department of Mechanical Engineering, Texas A&M University, College Station,  
Texas 77843-3123*

*A laser specklegram technique, or, equivalently, speckle photography, is capable of directly measuring local surface temperature gradients providing an extremely high resolution and a full-field interrogation from a single data taking. A complete specklegram system using a 35 mW power He-Ne laser has been developed at Texas A&M University, and the system has been applied to investigate heat transfer characteristics for a common configuration, but under some dispute in determining the heat transfer correlation. Convective heat transfer from an upward-facing isothermal plate has been studied by measuring the local and global Nusselt numbers. An aspect ratio (AR) of 1.75 has been considered in the present case. The Rayleigh number, based on the length scale equivalent to the ratio of the surface area to the perimeter, has varied from  $8.5 \times 10^4$  to  $2.0 \times 10^5$ . The results have been compared with several previously published calculations and data that employed classical and conventional techniques. The present result for the global heat transfer shows a 0.234 power law, i.e.,  $Nu = 0.46 Ra^{0.234}$ , correlates the data more properly, whereas previously published predictions and data for infinite or semi-infinite plate exhibit 0.2 power law. For the aspect ratios of order of unity, published correlations indicate that a 0.25 power law fit the data well. It is suggested that the band between 0.25 and 0.2 power correlations should contain the information for horizontal heated plates of AR ranging from 1.0 to  $\infty$  showing a gradual decrease in Nusselt number with increasing aspect ratio.*

### 1. INTRODUCTION

To determine the convective heat transfer coefficient of a heated surface, many well-established experimental techniques have been devised. These conventional techniques typically incorporate a conjugate heat transfer model or a mass transfer analogy. Whereas these experiments may be simple to construct and operate, several key assumptions or model mechanisms necessarily introduce gross simplifications and experimental bias. It is not uncommon, therefore, to see wide variations of results from researcher to researcher in the field of experimental heat transfer. This is due, for the most part, to the fact that classical experimental techniques for heat transfer measurements do not sufficiently represent the complex nature of convective heat transfer.

A conjugate heat transfer experiment involving a heated surface would normally determine the convective heat transfer coefficient in the following manner. By supplying a known power input to a heater element affixed to the plate, an energy balance can be written as:

$$q''_{\text{heater}} = q''_{\text{rad}} + q''_{\text{cond}} + q''_{\text{conv}} \quad (1)$$

NOMENCLATURE					
<i>a</i>	object distance, 2nd parabolic mirror	[m]	<i>P</i>	plate perimeter	[m]
<i>A</i>	plate surface area	[m <sup>2</sup> ]	<i>q''</i>	heat flux	$\left[\frac{W}{m^2}\right]$
<i>AR</i>	plate aspect ratio—	$\left[\frac{L}{W}\right]$	<i>Ra</i>	Rayleigh number	$\left[\frac{g\beta\Delta T x^3}{\nu\alpha}\right]$
<i>b</i>	image distance, 2nd parabolic mirror	[m]	<i>s</i>	fringe spacing	[cm]
<i>c</i>	camera defocal length	[cm]	<i>T</i>	temperature	[K]
<i>d</i>	distance to image plane from specklegram	[m]	<i>w</i>	plate width in photograph	[m]
<i>f</i>	mirror focal length	[mm]	<i>W</i>	actual plate width	[m]
<i>h</i>	local convective heat transfer coefficient	$\left[\frac{W}{m^2K}\right]$	<i>x</i>	characteristic length	$\left[\frac{A}{P}\right]$
$\bar{h}$	global convective heat transfer coefficient	$\left[\frac{W}{m^2K}\right]$	$\Delta$	speckle dislocation distance	[mm]
<i>k</i>	thermal conductivity	$\left[\frac{W}{mK}\right]$	<i>l</i>	laser wavelength, 632.8	[nm]
<i>L</i>	plate length (in LOS direction)	[m]	<b>Subscripts</b>		
<i>m</i>	image magnification		cond	conduction mode	
<i>m'</i>	camera magnification		conv	convection mode	
<i>n</i>	index of refraction, air		rad	radiation mode	
<i>Nu</i>	local Nusselt number	$\left[\frac{hx}{k}\right]$	heater	total input from heater	
$\bar{Nu}$	global Nusselt number	$\left[\frac{\bar{h}x}{k}\right]$	wall	property evaluated at wall temperature	
			<i>x</i>	direction parallel to plate surface	
			<i>y</i>	direction normal to plate surface	
			<i>z</i>	line of sight direction of laser	
			$\infty$	property evaluated at ambient conditions	

If one can completely eliminate heat conduction loss and entirely neglect radiation heat transfer, the convective heat transfer coefficient can be determined by directly measuring the plate surface temperature and the ambient temperature:

$$h = \frac{q''_{heater}}{[T_{wall} - T_{\infty}]} = \frac{q''_{conv}}{[T_{wall} - T_{\infty}]} \quad (2)$$

In reality, the conduction heat loss can never be completely eliminated and an empirical estimation of the conduction loss needs to be carefully assessed. Radiation losses are more difficult to assess and are usually neglected. It is not difficult to see the sources of errors and uncertainties for such a conjugate heat transfer experiment.

Mass transfer analogies, which incorporate Naphthalene (or similar substance) diffusion from a coated surface, also suffer from a critical source of error. In a mass transfer experiment, matter is diffusing away from the solid boundary. This necessarily introduces a nonzero flow velocity at the wall, one not present in an actual heat transfer experiment. Hence, the analogous heat transfer coefficient obtained from a mass transfer experiment is almost always overestimated.

To circumnavigate these difficulties, one can attempt to measure the convective heat transfer coefficient by measuring the wall temperature gradient. By equating the entirely

conduction heat transfer at the wall with the mostly convection heat transfer away from the wall, the heat transfer coefficient can be expressed in terms of wall temperature gradient and other known or readily measurable parameters:

$$h = \frac{q''_{\text{cond,wall}}}{[T_{\text{wall}} - T_{\infty}]} = \frac{-k \left[ \frac{\partial T}{\partial y} \right]_{y=0}}{[T_{\text{wall}} - T_{\infty}]} \quad (3)$$

Here, the radiation heat transfer is invariant in both the conduction and the convection regime and the radiation effect is decoupled from the heat balance. Nonintrusive optical techniques allow the measurement of wall temperature gradients without disturbing fluid flow.

Of all the nonintrusive methods for temperature gradient, interferometry has clearly received the most attention. However, an equally effective, if not superior yet not as highly recognized, method employs laser speckle photography. Although both methods share the same basic principles of light refraction through an anisotropic density field, the specklegram technique holds several distinct advantages over laser interferometry. The most notable advantage is the specklegram's excellent spatial resolution. Whereas an interferometer has a limited accuracy dictated by the number of fringes present in an interferogram and the ability to count integral fringe "shifts," the specklegram's accuracy is limited only by the distance between two laser speckles on the photographic plate, which is on the order of microns.

The present experimental study focuses on determining the variation of local and global Nusselt numbers for an upward facing, horizontal-heated plate. Heat transfer from a horizontal-heated plate is inherently less stable because of the downflow of cold fluid toward the heated plate. The current consensus among researchers is that a power law relationship predicts the heat transfer correlation as:

$$Nu = C_1 Ra^n \quad (4)$$

where the exponent,  $n$ , ranges from 0.20 to 0.25 and the constant,  $C_1$ , could range anywhere from 0.4 to 0.8, depending on the Rayleigh number range and plate geometry. Fishenden and Saunders [2] found  $C_1$  to be 0.38 using the 1/4 power, whereas Goldstein et al. [5] found  $C_1$  to be 0.59. Goldstein et al. [4,5] later suggested 0.75 and 0.83 for  $C_1$  while using a 1/5 power. Other results that yielded similar power law expressions include rectangular geometries with aspect ratios ranging from 2.0 [10] to 7.0 [5].

Very few attempts have been made to study the problem using nonintrusive optical techniques. Pera and Gebhart [12] employed Mach-Zehnder interferometry to find that the thermal boundary layer above the heated plate was frequently irregular in shape, fluctuating in time, and did not always separate at the same location. Kihm and Cheeti [7] recently used the laser specklegram technique to analyze a horizontal plate of high aspect ratio (AR) of 15 in order to simulate a 2-D plate with infinite aspect ratio. This geometry was selected such that the results could be compared with theoretical and numerical work, all of which assumed an infinitely long heated plate. The results of Kihm and Cheeti [7] exhibited fairly good agreement with these predictions, showing 1/5 power correlation and the constant  $C_1$  within the range of the predicted values. Previous experimental work, however, used rectangular geometries with aspect ratios of order of unity, and their

results generally showed higher Nusselt numbers compared with the case of  $AR = 15$  [7].

In an attempt to investigate the discrepancies between the previous predictions and experiments, a rectangular-shape, heated plate with an aspect ratio close to one is employed in the present study that uses a laser specklegram technique as a measurement tool for the wall temperature gradient.

## 2. EXPERIMENTAL PROCEDURE

Perhaps the foremost and most complete description of speckle photography can be found in Françon [3]. The technique has been applied to various heat convection problems and showed high accuracy and convenience [6,11]. As a detailed description of the speckle photography system used for the study is available in Kihm and Cheeti [7], only an essential feature of the technique is summarized.

Fraunhofer diffraction results from regular constructive and destructive interference from two rectangular slits at a finite distance apart (Fig. 1). Speckle diffraction, in contrast, results from coherent laser light impinging on a random diffraction grating. That is, the grating consists of randomly sized and oriented slits, which in turn causes a random interference pattern of bright and dark "spots," or speckles (Fig. 2). A piece of plate glass that has been sandblasted on one side typically serves as the random diffraction grating. When a heated test section is placed in front of the ground glass, the incoming light rays are refracted due to the change of index of refraction of the warmer air. This shifting of the incoming laser light causes the speckles in the random diffraction pattern to shift a small, finite amount  $\Delta$ . Hence if one can measure the local dislocation of speckles, one can calculate the change of index of refraction of the air at a given point in the test section. From that, the density gradient, or the associated temperature gradient, can be determined at that point.

The speckle photography system is shown schematically in Fig. 3A. Double-exposed recording, with and without the test section present, constructs a speckle photograph. Figure 3B illustrates the scheme that evaluates the speckle distance indirectly from the measurement of the Young's fringes generated by illuminating the specklegram with a (secondary) laser beam. The temperature gradient can now be expressed as [6]:

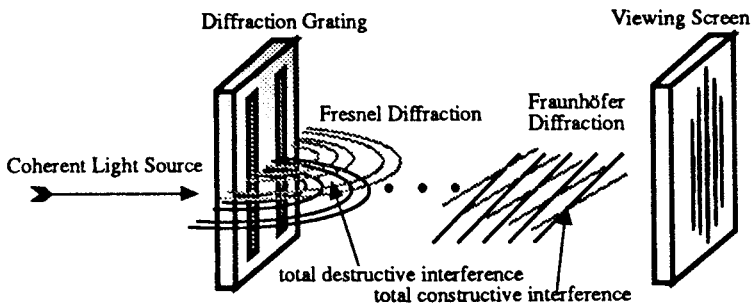


Fig. 1 Fraunhofer diffraction pattern.

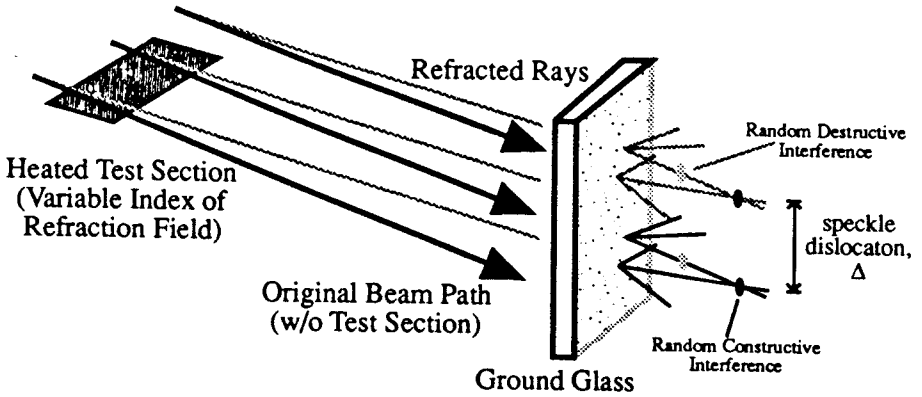


Fig. 2 Speckle dislocation from a random diffraction pattern.

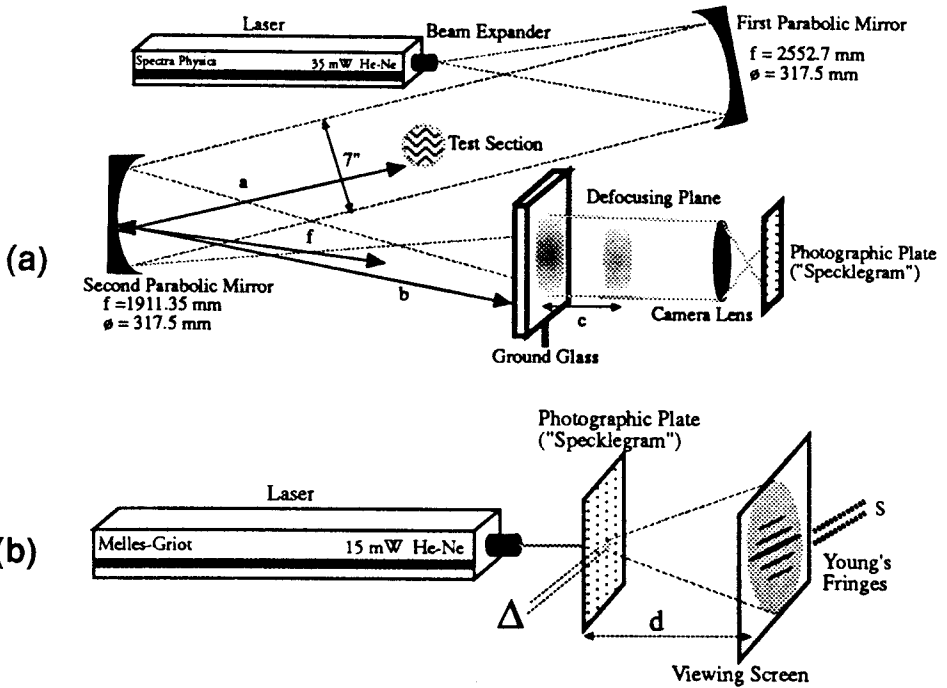


Fig. 3 Experimental apparatus-general schematic (A); Experimental apparatus-speckle dislocation evaluation (B).

$$\frac{\partial T}{\partial y} = \frac{\lambda d}{Lcs} \frac{m}{m'} \left( \frac{\partial n}{\partial T} \right)^{-1} \quad (5)$$

where the  $y$ -direction is normal to the plate. The change of index of refraction of air with respect to change in temperature is given as a function of temperature [13]. With specified magnifications,  $m$  and  $m'$  for the schlieren head and the camera, and known optical and

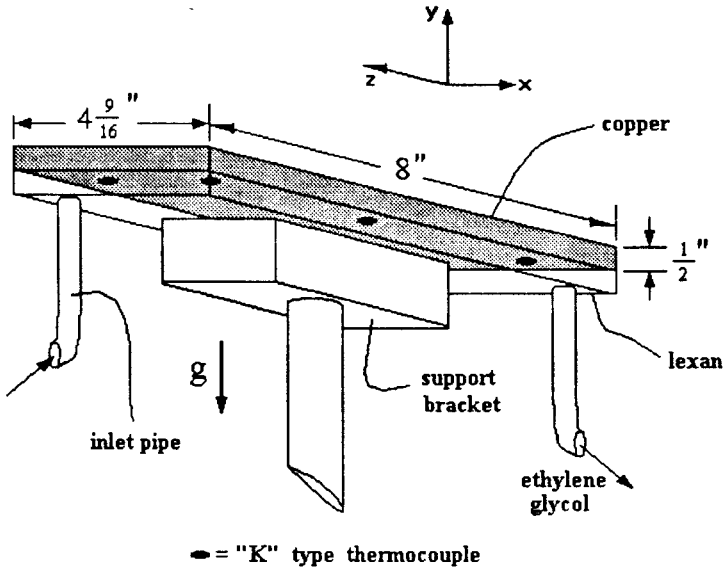


Fig. 4 Test section schematic.

geometrical parameters, the fringe spacing,  $s$ , remains to be determined to know the temperature gradient. The local heat transfer coefficient at a point can then be calculated by substituting values of the temperature gradient of Eq. (5) into Eq. (3). Additionally, all speckles have a statistically dominant direction of dislocation in parallel to the primary heat transfer direction. Thus the normal direction to the fringe layers always indicate the dominant direction of heat transfer.

One of the best features of the speckle photography technique is that a single specklegram provides a full-field interrogation of the test section. Since the specklegram system deals with speckle dislocations on a statistical average, the system is not as sensitive to vibration as many other laser optical techniques. Thus the specklegram system is much cheaper to operate than interferometric experiments, and experimental uncertainties can be anticipated to be less than  $\pm 5\%$  [9]. In the present research, an uncertainty analysis yielded an average error in global Nusselt number of  $\pm 7.75\%$ .

A rectangular copper plate, 116 mm wide and 203 mm long in the line-of-sight direction, with a grooved channel on the back for circulating heated fluid is used to provide a heated plate (Fig. 4). The grooved rear surface was covered with a 1-cm-thick Lexan plate to serve as a fluid jacket. Heated ethylene glycol was pumped through the plate jacket from a constant temperature bath and the plate surface temperature was monitored from 9 K-type thermocouple probes, mounted inside the plate within 1 mm from the surface, and spread uniformly about the plate. Once the surface temperature of the plate had reached steady-state, the plate temperature was found not to vary more than  $\pm 0.2^\circ\text{C}$  over the thermocouple readings across the plate. The ambient temperature was also monitored by a K-type thermocouple and was found to remain nearly unchanged during the data taking period.

The local heat transfer coefficient was evaluated at 10 different locations along the

width of the plate under a constant surface temperature. The 10 measurements were then integrated to determine the global heat transfer coefficient and the subsequent Nusselt number. The Rayleigh number, which is based on the length scale defined as the ratio of the surface area to the perimeter length, ranged from  $8.5 \times 10^4$  to  $2.0 \times 10^5$ .

### 3. RESULTS

Rising heated air mixing with descending cooler air above an upward facing heated plate causes thermal plumes, or convection "rolls," which are naturally unstable and irregularly developing. It is then expected that the thermal boundary layer above the plate should fluctuate with time. However, these unstable and irregular features of the thermal flow above the plate will drastically diminish as the plate wall is approached. Thus values of wall temperature gradients, which are measured using the specklegram technique, are expected to have far less fluctuations and maintain a fair level of stability.

Figure 5 shows the variations of local fringes across the width of the plate for two different Rayleigh numbers. A low local heat transfer coefficient is characterized by a gradual temperature gradient and widely spaced fringes (Fig. 5a), and a high heat transfer coefficient will have fringes closely spaced (Fig. 5b). For the lower Rayleigh number case, the fringes are oriented diagonally right at the edge of the plate and vary smoothly

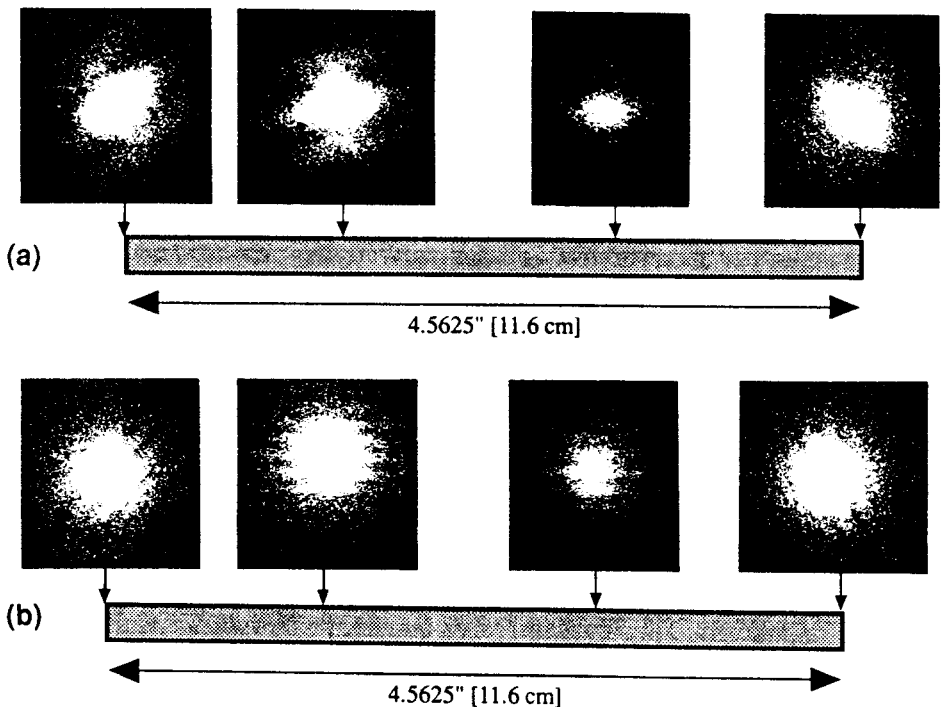


Fig. 5 Temperature gradient across plate span [ $Ra = 8.5 \times 10^4$ ] (A); temperature gradient across plate span [ $Ra = 2.0 \times 10^5$ ] (B).

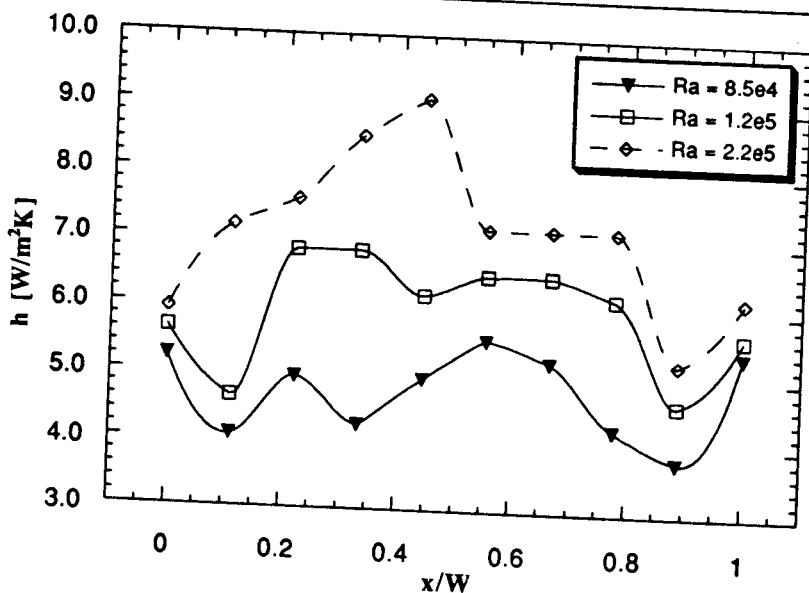


Fig. 6 Local heat transfer coefficient vs. spanwise location.

toward the centerline. This is as one might expect for a more steady, less fluctuating case. For the higher Rayleigh number, the fringes show the same edge orientation, but then vary more sharply toward the center. But the slope of the fringes are symmetric about the middle of the plate, where the highest heat transfer coefficient is expected. This provides some evidence for the existence of a thermal plume both near the center of the plate and at the edge.

Figure 6 shows the variation of local heat transfer coefficient across the width of the plate for a range of representative Rayleigh numbers. As expected, higher Rayleigh number flows give consistently higher local Nusselt numbers. Also of note is the convective heat transfer taking place along the edges of the plate. Within the first 20% of either edge, all cases maintain the same general profile; high heat transfer at the edge, followed by a sharp drop in  $h$ , and then a strong recovery. This would be indicative of a strong thermal plume along the outer surface. Furthermore, for the lower Rayleigh numbers, the heat transfer coefficient remains relatively constant over the middle 60% of the plate. When the quantitative information from Fig. 6 is combined with the qualitative knowledge from the fringe patterns in Fig. 5a,b, one can complete a picture of the overall heat transfer behavior.

Figure 7 shows the global Nusselt number plotted over the range of Rayleigh numbers considered. Also plotted on the same graph is the recent data for a rectangular plate with very high aspect ratio,  $AR = 15$ , by Kihm and Cheeti [7]. These previous data show excellent agreement with the predictions of Bandrowski and Rybski [1], which represent the numerical work of the similarity solution for an infinite plate ( $AR \rightarrow \infty$ ) employing a mass transfer analogy. For such cases of high or infinite aspect ratios, a  $1/5$  power law well describes the correlation between Nusselt number and Rayleigh number.



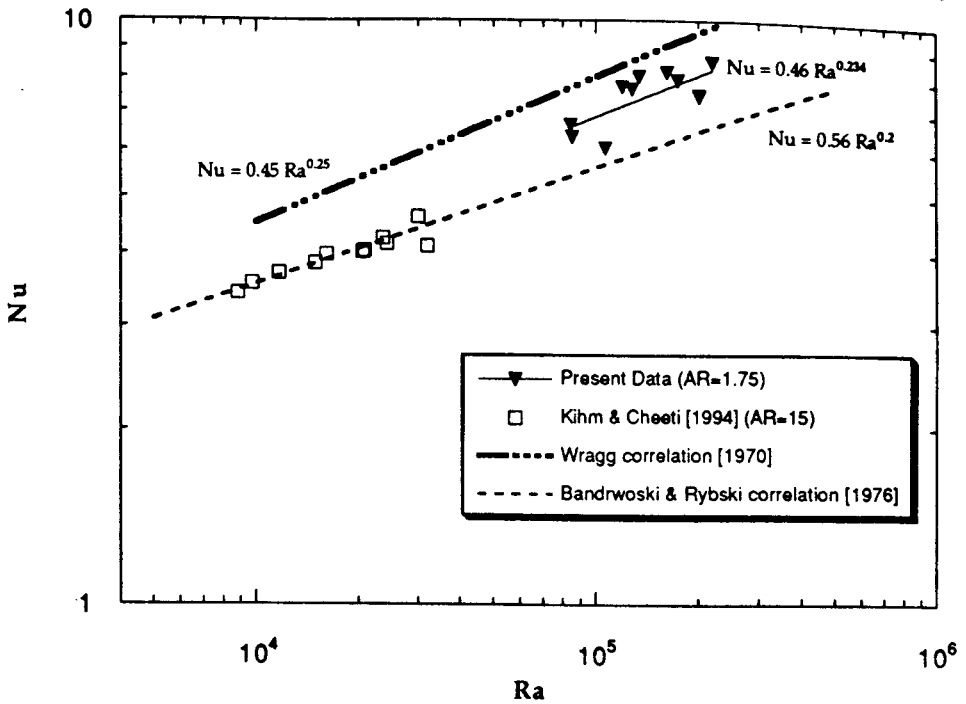


Fig. 7 Comparison of experimental results.

The upper dashed line in Fig. 7 represents the correlation proposed by Wragg and Loomba [14] that fit their experimental data obtained using an electrochemical method. These researchers employed square and circular geometries and proposed a  $1/4$  power law for the correlation.

The present data falls in between the results representing the 2-D infinite plate and the electrochemical experiments. Wragg and Loomba's experiments [14], which is basically a mass transfer analogy, could very well be an overprediction of the true mechanism due to the nonzero wall velocity imposed. The current research, which employs a geometry with  $AR = 1.75$ , falls uniformly below the mass transfer experiment. However, the present data fall above the 2-D result. Again, this would be as expected because the square geometry has larger edge perimeter length per surface area and the local Nusselt number along the edge is usually above average due to the larger temperature differential between the heated surface and the cold inflow. The present results fall completely within a band of correlations between  $1/5$  power law and  $1/4$  power law correlations. In fact, a power law correlation,  $Nu = 0.46 Ra^{0.234}$ , fits the present data. It is also suggested that the band between  $1/4$  and  $1/5$  power should contain the information for horizontal heated plates of  $AR$  ranging from 1.0 to  $\infty$ , showing a gradual decrease in Nusselt number with increasing aspect ratio.

The traditionally accepted length scale used for the Nusselt and Rayleigh numbers is defined as the ratio of the surface area to the edge perimeter length. The length scale

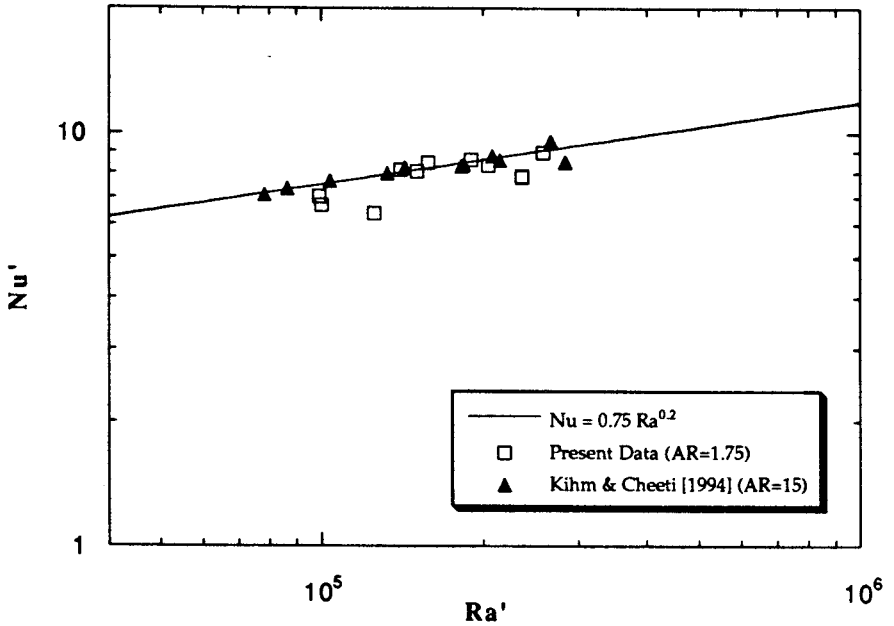


Fig. 8 Recent data— $Nu'$  vs.  $Ra'$ .

and surface area of the plate used in the present experiment are 36.9 mm and 24,013 mm<sup>2</sup>, respectively. Kihm and Cheeti [7] tested a plate of length scale and area of 18.7 mm and 24,000 mm<sup>2</sup>, respectively. If the characteristic length scale is newly defined as  $x' = \frac{\sqrt{A}}{4}$ , 1/4 of the square root of the heated surface area, both cases have basically the exact same length scale,  $x' = 38.7$  mm. When the same data from Fig. 7 are replotted by redefining the Nusselt and Rayleigh numbers as  $Nu'$  and  $Ra'$  based on  $x'$ , both the present and Kihm and Cheeti's data [7] collapse into a single correlation,  $Nu' = 0.75 Ra'^{0.2}$  (Fig. 8). Although this may be just an experimental coincidence, it does raise an intriguing question on whether there exists a more comprehensive manner in defining the heat transfer coefficients. In exploring this, the suggested length scale,  $x'$ , certainly has a positive argument in that the heat transfer of an upward facing surface should be proportional to a significant degree to the heated surface area.

#### 4. CONCLUSIONS

It has been shown that a laser specklegram technique can successfully determine local convective heat transfer coefficients of an upward-facing horizontal heated plate. Upon analyzing data from the current research and comparing it with similar results

from other experimental and numerical work, three basic trends and conjectures can be made:

1. The local heat transfer coefficient,  $h$ , is seen to increase monotonically with Rayleigh number across the span of the plate. Lower Rayleigh numbers tend to exhibit a more uniform heat transfer coefficient profile. It was also seen that edge effects of heat transfer coefficient maintain a similar shape regardless of Rayleigh number. That is, high heat transfer is seen right at the plate edge, followed by a sharp drop as one moves inward along the plate. Then, the heat transfer coefficient recovers to obtain a maximum value somewhere in the inner portion of the plate. This type of edge effect occupies roughly 40% of the spanwise heat transfer area.
2. Present data for  $Nu$  vs.  $Ra$  for  $AR = 1.75$  falls directly between the 2-D numerical and experimental results and the correlation obtained from a mass transfer analogy experiment using a square geometry. Previously published results list a power law relation between Nusselt number and Rayleigh number, where the exponent ranges from  $1/4$  to  $1/5$ . The present data follows  $Ra^{0.234}$  power correlation.
3. An interesting trend is seen between the present specklegram data, and the ones obtained by Kihm and Cheeti [7]. If both sets of data are plotted using a new characteristic length scale,  $x' = \frac{\sqrt{A}}{4}$ , both sets of data collapse to a single curve,  $Nu' = 0.75 Ra'^{0.2}$ . Although this result is not intended to redefine the length scale for heat transfer experiments, it does raise the possibility of condensing the vast amount of experimental heat transfer data.

The third conjecture obviously suggests that more encompassing experimental work be done to validate the existence of such a new length scale. This would require many experiments to be run on plates of varying aspect ratio and Rayleigh number range. Furthermore, to even more accurately predict the complex mechanisms of convective heat transfer on heated plates of low aspect ratio, one must begin to look toward 3-D optical techniques for flow evaluation. This means that the current specklegram system must be updated to perform tomographic experiments. Such work is currently under study.

## REFERENCES

1. J. Bandrowski, and W. Rybski, Free Convection Mass Transfer from Horizontal Plates, *Int. J. Heat Mass Transfer*, vol. 19, pp. 827-838, 1976.
2. M. Fishenden, and O. A. Saunders, *An Introduction to Heat Transfer*, pp. 95-97, Oxford University Press, London, pp. 95-97, 1950.
3. Françon, M., *Laser Speckle and Applications in Optics*, Academic Press, New York, pp. 1-161, 1979.
4. R. J. Goldstein, and K.-S. Lau, Laminar Natural Convection from a Horizontal Plate and the Influence of Plate-Edge Extensions, *Journal of Fluid Mechanics*, vol. 129, pp. 55-75, 1983.
5. R. J. Goldstein, E. M. Sparrow, and D. C. Jones, Natural Convection Mass Transfer Adjacent to Horizontal Plates, *Int. J. Heat Mass Transfer*, vol. 16, pp. 1025-1035, 1973.
6. D. Kastell, K. D. Kihm, and L. S. Fletcher, Study of Laminar Thermal Boundary Layers

- Occurring around the Leading Edge of a Vertical Isothermal Wall using a Specklegram Technique, *Experiments in Fluids*, vol. 13, pp. 249–256, 1992.
7. K. D. Kihm, and S. K. R. Cheeti, Study of Thermal Flows from Two-Dimensional, Upward-Facing Isothermal Surfaces using a Laser Speckle Photography Technique, *Experiments in Fluids*, 1994 (accepted).
  8. K. D. Kihm, Image Blurring of Test Section Boundary in a Specklegram Technique for Temperature Gradient Measurements, *Applied Optics*, vol. 31, no. 28, pp. 5907–5910, 1992.
  9. K. D. Kihm, J. H. Kim, and L. S. Fletcher, Investigation of Natural Convection Heat Transfer in Converging Channel Flows Using a Laser Specklegram Technique, *ASME Journal of Heat Transfer*, vol. 115, no. 1, pp. 140–148, 1992.
  10. J. R. Lloyd, and W. R. Moran, Natural Convection Adjacent to Horizontal Surfaces of Various Planforms, *ASME Journal of Heat Transfer*, vol. 96, pp. 443–447, 1974.
  11. W. Merzkirch, Density-Sensitive Whole-Field Flow Measurement by Optical Speckle Photography, 3rd Int'l Conf. on Experimental Heat Transfer, Fluid Mechanics and Thermodynamics, Honolulu, HI, 1993.
  12. L. Pera, and B. Gebhart, Natural Convection Boundary Flow over Horizontal and Slightly Inclined Surfaces, *Int. J. Heat Mass Transfer*, vol. 16, pp. 1131–1146, 1973.
  13. C. M. Vest, *Holographic Interferometry*, John Wiley & Sons, New York, pp. 344–345, 1979.
  14. A. A. Wragg, and R. P. Loomba, Free Convection Flow Patterns at Horizontal Surfaces with Ionic Mass Transfer, *Int. J. Heat Mass Transfer*, vol. 113, pp. 439–442, 1970.